

1 **Research Paper**

2

3 **Title**

4 Population dynamics and disease-linked host use of the sea urchin symbiont *Dactylopleustes*  
5 *yoshimurai* (Crustacea: Amphipoda: Pleustidae) on *Strongylocentrotus intermedius*

6

7 **Running head**

8 Population dynamics of *Dactylopleustes yoshimurai*

9

10 **Authors**

11 Masafumi Kodama, Ryoga Yamazaki, Ko Tomikawa, Gen Kume, Toru Kobari, Jun Hayakawa

12

13 **Corresponding Author**

14 Masafumi Kodama

15 E-mail: [mkodama@fish.kagoshima-u.ac.jp](mailto:mkodama@fish.kagoshima-u.ac.jp)

16

17

18 **Abstract**

19 *Dactylopleustes yoshimurai* is an echinoid-associated amphipod that frequently aggregates on disease  
20 lesions of the short-spined urchin *Strongylocentrotus intermedius* in Otsuchi Bay, northeastern Japan.  
21 However, its life history and use of diseased hosts remain poorly understood. We combined four years  
22 of monthly SCUBA surveys (Jan 2020–Jan 2024) with quantitative sampling of diseased and healthy  
23 urchins (Jan 2021–Jan 2024) to examine how host disease status structures the population dynamics  
24 of *D. yoshimurai*. The amphipod occurred on ~10–80% of urchins and was consistently more frequent  
25 and much denser on diseased than on healthy hosts, with winter peaks that broadly coincided with  
26 maxima in disease prevalence. Size–frequency distributions on diseased urchins were strongly  
27 dominated by juveniles (<2.5 mm), especially in winter to early spring, whereas healthy urchins  
28 supported low densities but a relatively higher proportion of adults. Ovigerous females were rare but  
29 occurred mainly in late summer and autumn on both host types, and juvenile pulses in winter, together  
30 with the year-round presence of small juveniles, indicate an extended reproductive period with a  
31 seasonal peak in late summer–autumn and recruitment continuing into winter. These results show that  
32 host disease status and amphipod life history jointly shape the population dynamics of *D. yoshimurai*,  
33 and highlight lesions on urchins as seasonally dynamic habitat patches that are particularly important  
34 for juvenile stages.

35

36

37 **Keywords**

38 *Dactylopleustes yoshimurai*; sea urchin symbiont; bald sea urchin disease; population dynamics;  
39 host–symbiont interactions

40

41 ■ **Introduction**

42 The order Amphipoda is one of the largest crustacean orders, comprising more than 10,000  
43 described species (Horton et al. 2025, Lowry & Myers 2017). Symbiotic associations with various  
44 other animals have been well documented across the group (e.g., Vader, 1978, 1983; Vader &  
45 Tandberg, 2013, 2015; Iwasa-Arai & Serejo, 2018; Tomikawa *et al.*, 2019; Kodama *et al.*, 2022;  
46 Hanaoka *et al.*, 2025). However, for many host-specialized amphipods, basic aspects of ecology and  
47 life history remain poorly documented.

48 Amphipods of the genus *Dactylopleustes* Karaman & Barnard, 1979 (Amphipoda: Pleustidae)  
49 are known as symbionts of sea urchins and are thought to have evolved adaptations for living on the  
50 host's body surface (Vader, 1978; Bousfield & Hendrycks, 1995). Despite this close association, basic  
51 information on the ecology and life history of *Dactylopleustes* species is still limited (Vader, 1978),  
52 and it remains unclear whether these amphipods affect their host urchins.

53 *Dactylopleustes yoshimurai* Tomikawa, Hendrycks & Mawatari, 2004 occurs on the body  
54 surface of sea urchins including *Strongylocentrotus intermedius* (Tomikawa *et al.*, 2004; Kodama *et*  
55 *al.*, 2020). Recent field observations further showed that *D. yoshimurai* frequently aggregates on  
56 disease lesions of host urchins, while comparable aggregations are not observed on healthy urchins  
57 (Kodama *et al.*, 2020). These aggregations are often dominated by small juveniles, whereas juveniles  
58 are rarely found on healthy urchins. This pattern has been interpreted as that amphipods feed on  
59 exposed host tissues at lesions (Kodama *et al.*, 2020). However, DNA metabarcoding of gut contents  
60 suggested that even aggregated individuals contained only a limited proportion of urchin-derived  
61 material and instead relied heavily on non-host resources such as sediments (Kodama *et al.*, 2024).  
62 Though both the importance of aggregation and the life-stage dependence of host use remain  
63 unresolved, aggregations on lesions have been observed repeatedly and with high consistency,  
64 suggesting that this behavior may have important implications for the life history of this species.  
65 Nevertheless, the basic life history of the species remains unclear, and it is also unknown when and  
66 how, within its life cycle, the amphipods used diseased host urchins.

67 The present study aims to clarify (i) the basic life history and seasonal population dynamics of  
68 *D. yoshimurai* on its host urchins and (ii) how host disease status is associated with amphipod density  
69 and demographic structure. To address these aims, we conducted monthly SCUBA surveys in order  
70 to quantify body length, sex, and maturity stage, as well as the number of amphipods per a diseased  
71 and healthy *S. intermedius*. By comparing amphipod population characteristics between diseased and  
72 healthy hosts across seasons, we evaluate when (and which life stages of) *D. yoshimurai* are most  
73 strongly associated with diseased urchins.

75 ■ Materials and Methods

76 **Field survey and sampling**

77 This study was carried out in a rocky subtidal area at Akahama in Otsuchi Bay, Japan (Figs. 1:  
78 39°21'00" N, 141°56'10" E, 2–3 m deep). Monthly field survey using SCUBA was conducted from  
79 Jan 2020 to Jan 2024, except for the following months: Oct 2021; Nov, Dec 2022; Feb, Nov 2023. At  
80 each monthly survey, 50 individuals of the short-spined sea urchin *Strongylocentrotus intermedius*  
81 were randomly selected. For each urchin, we recorded the test diameter, and visually recorded (i) the  
82 presence or absence of visible disease lesions and (ii) the presence or absence of visible  
83 *Dactylobleustes yoshimurai*.

84 To obtain an index of urchin availability/density during each survey, we recorded the elapsed  
85 time required to locate and measure 50 individuals and calculated catch per unit effort (CPUE;  
86 individuals h<sup>-1</sup>) as: CPUE = 50 / survey time (h). Because the number of processed individuals was  
87 fixed, higher CPUE indicates a shorter search/processing time and thus greater local availability of  
88 urchins. CPUE could not be calculated for months in which the end time was not recorded.

89 The urchin's disease found in Otsuchi Bay appears to be a kind of bacterial disease called 'bald  
90 sea urchin disease' (Johnson, 1971, Shaw *et al.*, 2023). However, it is impossible to identify the causes  
91 of disease in the field. In this study, therefore, a 'diseased urchin' was defined as an urchin with the  
92 following symptoms following Kodama *et al.* (2024): an area of the test without spines and tube feet,  
93 exposing the surface tissue discoloured to deep purple or black. These symptoms are typical of bald  
94 sea urchin disease.

95 At the SCUBA surveys from Jan 2021 to Jan 2024 except for Apr 2022, Jun and Aug 2023, six  
96 diseased individuals and six healthy individuals of *S. intermedius* were haphazardly collected,  
97 respectively, from the area neighboring the area for the above monitoring survey. Each urchin  
98 individual was gently placed in plastic bags to prevent escape of symbiotic organisms. The urchins  
99 and its symbionts were all anaesthetized with iso-osmotic 7.5% weight% magnesium chloride  
100 (MgCl<sub>2</sub>.6H<sub>2</sub>O). Then, *D. yoshimurai* detached from the urchins by anesthesia were counted and  
101 preserved in 80% ethanol.

102 Seasonal fluctuation in the number of *D. yoshimurai* on an urchin was assessed and visualized  
103 using generalized additive models (GAMs) with the 'mgcv' package in R. The sampling months were  
104 treated as explanatory factor. Negative binomial distribution was used in GAM. Sampling month data  
105 were transformed into the number of elapsed months from the first sampling and thus treated as a  
106 continuous data set (not categorical data).

107 To examine whether host body size influences the occurrence of lesions and/or amphipod  
108 association (i.e., potential size-based host preference), each urchin was assigned to one of four

109 categories based on the combination of lesion status and amphipod occurrence: (1) healthy urchins  
110 without amphipods observed, (2) healthy urchins with amphipods observed, (3) diseased urchins  
111 without amphipods observed, and (4) diseased urchins with amphipods observed. Differences in test  
112 diameter among the four groups were evaluated using a Kruskal–Wallis rank-sum test. When the  
113 overall test was significant, pairwise comparisons were conducted using Dunn’s test with Bonferroni  
114 adjustment for multiple testing. The analyses were performed using the package “dunn.test” in R.  
115

116

### 117 **Sample processing in the laboratory**

118 A total of 1,899 *D. yoshimurai* individuals were collected between January 2021 and January 2024.  
119 Eleven individuals were damaged and thus excluded from the measurement, leaving 1,888 individuals  
120 for analysis about body length. Body length was measured from the tip of rostrum along the dorsal  
121 margin to the posterior margin of telson (measurements were done on the curved body). The  
122 determination of sex and developmental stage was based on the presence or absence of oostegites  
123 (females) and of genital papillae (males). Females were first classified as ovigerous or non-ovigerous  
124 based on the presence or absence of eggs. Non-ovigerous females were then examined for setation  
125 on the oostegites: individuals lacking eggs but bearing well-developed and setose oostegites were  
126 classified as mature females, whereas those with oostegites that were present but not setose were  
127 classified as immature females. Individuals without oostegites or genital papillae were considered  
128 juveniles.

129

130

## 131 ■ Results

### 132 **Temporal variation in host disease and occurrence of *Dactylopleustes yoshimurai***

133 *Dactylopleustes yoshimurai* was frequently found on the short-spined urchin *Strongylocentrotus*  
134 *intermedius* throughout the study period (Fig. 2). The proportion of urchins bearing *D. yoshimurai*  
135 ranged from about 10% to about 80% of the 50 individuals examined per month and was usually  
136 >20%. Peaks in occurrence (>60% of urchins with amphipods) were typically observed in winter (e.g.  
137 late 2020, late 2021–early 2022, late 2022 and late 2023), although elevated values also occurred  
138 sporadically in other seasons.

139 The proportion of urchins showing lesions (“bald sea urchin disease”) was generally lower and  
140 showed more distinct seasonality than amphipod occurrence, fluctuating between 0 and about 40%  
141 (Fig. 2). Disease prevalence tended to increase in late autumn and winter each year, with conspicuous  
142 peaks in 2020–2021, 2021–2022 and 2023–2024, whereas it was usually <10% in late spring and

143 summer. In most years, periods of high disease prevalence overlapped with peaks in the proportion  
144 of urchins bearing *D. yoshimurai* (Fig. 2).

145 Urchin availability, indexed by CPUE, remained broadly stable throughout the monitoring  
146 period (Fig. 2). The CPUE were typically around  $\sim$ 100 individuals  $h^{-1}$  (median 93.8; mean 95.6),  
147 ranging from 46.2 individuals  $h^{-1}$  (Apr 2022) to 176.5 individuals  $h^{-1}$  (Apr 2021). Although  
148 occasional months showed moderately high or low values, CPUE remained broadly stable over time  
149 and no clear seasonal pattern in CPUE was apparent.

150 Test diameter differed among the four groups (Fig. 3; Kruskal–Wallis:  $\chi^2 = 17.29$ ,  $df = 3$ ,  $p <$   
151 0.001;  $\varepsilon^2 = 0.006$ , indicating a small effect). Post-hoc Dunn's tests with Bonferroni correction detected  
152 a significant difference only between healthy urchins without amphipods observed and diseased  
153 urchins without amphipods observed (adjusted  $p = 0.0024$ ), whereas all other pairwise comparisons  
154 were not significant (adjusted  $p > 0.05$ ). Median test diameter was 43.30 mm in healthy urchins  
155 without amphipods and 46.15 mm in diseased urchins without amphipods (median difference = 2.85  
156 mm), with substantial overlap in interquartile ranges. The test diameter distribution consistently  
157 peaked at 40–50 mm in all months, and no clear seasonal shift was detected (Fig. 4).

158

#### 159 ***Temporal variation in number of Dactylobleustes yoshimurai on diseased and healthy urchins***

160 From January 2021 to January 2024, a total of 348 urchins (six diseased and six healthy urchins per  
161 sampling) were collected for quantitative counts of *D. yoshimurai*. A total of 1,899 amphipods were  
162 collected, of which 1,696 were from diseased urchins and 203 were from healthy urchins.

163 The number of *D. yoshimurai* on an urchin differed strikingly between diseased and healthy  
164 urchins. Diseased urchins often hosted dense aggregations, with up to about 100 individuals on a  
165 single host and many samples exceeding 20 individuals per urchin (Fig. 3). In contrast, healthy  
166 urchins typically bore only a few amphipods (0–5 individuals per urchin), and hosts without an  
167 amphipod were common. As a result, the fitted GAM for the number of *D. yoshimurai* on an urchin  
168 showed consistently higher values for diseased than for healthy urchins throughout the study period  
169 (Fig. 3).

170 The number of *D. yoshimurai* on diseased hosts also exhibited pronounced seasonal variation  
171 (Fig. 3). Large numbers of amphipods were observed on diseased urchins in winter of each year.  
172 Between these peaks, the number of amphipods on diseased hosts dropped to low values in late spring  
173 and summer. By contrast, the fitted GAM for healthy urchins remained close to zero across all months,  
174 with only minor seasonal fluctuations and no conspicuous peaks (Fig. 3).

175

#### 176 ***Size structure and demographic composition of Dactylobleustes yoshimurai on diseased urchins***

177 Body length of *D. yoshimurai* ranged from ca. 0.5 to 7.0 mm (Figs. 4, 5). On diseased urchins, the  
178 assemblage was dominated by juveniles in most months (Fig. 4). Large numbers of small juveniles  
179 (body length <2.5 mm) occurred repeatedly in winter to early spring (e.g. January–March 2021,  
180 January 2022, January 2023, December 2023–January 2024), forming distinct unimodal peaks at  
181 small size classes. Although small juveniles appeared repeatedly in winter to early spring, the  
182 subsequent progression of distinct cohorts was not always clear, as size–frequency distributions often  
183 overlapped among months and did not consistently show a smooth modal shift.

184 Adult size classes (mature females, ovigerous females and males, generally > 4.0 mm) were  
185 present on diseased urchins in many months but always occupied small proportions of the total  
186 assemblage (Fig. 4). Ovigerous females (dark red bars) were detected intermittently, most frequently  
187 from late spring to autumn (e.g. May–July 2021, February–June 2022, and sporadically in 2023), and  
188 were usually among the largest individuals in the population (5–7 mm; arrows in Fig. 4). Mature but  
189 non-ovigerous females and adult males were also concentrated in these larger size classes.

190  
191 **Size structure and demographic composition of *Dactylopleustes yoshimurai* on healthy urchins**  
192 On healthy urchins, *D. yoshimurai* occurred at much lower numbers, and the size–frequency  
193 distributions therefore contained fewer individuals per month (Fig. 5). Juveniles were present in many  
194 months but usually only in small numbers (typically fewer than five individuals per size class). Adult  
195 males and females, including ovigerous females, were observed intermittently across years. Only five  
196 ovigerous females were recorded on healthy urchins, and thus the timing of reproduction cannot be  
197 determined conclusively. However, ovigerous females on healthy urchin were most frequently  
198 observed in late summer and early autumn (e.g. August–September 2021, September–October 2022,  
199 and September 2023; arrows in Fig. 5). This seasonal tendency is broadly consistent with the pattern  
200 observed on diseased urchins and supports the inference that reproduction likely peaks from late  
201 summer to autumn.

202 Although the total number of amphipods on healthy urchins was small, the coexistence of  
203 juveniles and adults including ovigerous females in some months indicates that all life stages can  
204 occur on healthy hosts. Nevertheless, in contrast to diseased urchins where juveniles overwhelmingly  
205 dominated, the smaller assemblages on healthy urchins were often comprised of a relatively higher  
206 proportion of adults (Fig. 5).

207  
208  
209 **■ Discussion**  
210 Our four-year survey revealed that the population dynamics of the urchin symbiont *Dactylopleustes*

211 *yoshimurai* differ markedly between diseased and healthy hosts and show a distinct seasonal pattern.  
212 On healthy *Strongylocentrotus intermedius*, the amphipod occurred at low densities (number of  
213 individuals per an urchin) throughout the year, whereas diseased urchins supported dense  
214 aggregations, particularly in winter. These patterns closely paralleled seasonal changes in the  
215 prevalence of “bald sea urchin disease”, which increased in late autumn and winter and declined in  
216 late spring and summer (Fig. 2; see also Johnson, 1971; Shaw *et al.*, 2023; Kodama *et al.*, 2024).  
217 These results indicate that *D. yoshimurai* uses host lesions that are most frequent in winter as key  
218 habitat patches within its life cycle, while also persisting at low densities on healthy urchins year-  
219 round.

220 The “diseased” urchins in this study were defined by characteristic symptoms (the spines are  
221 observed to have fallen off in an area of the test, exposing the tissue, which is black and discolored)  
222 that are typical of bald sea urchin disease (Johnson 1971; Shaw *et al.*, 2023; Kodama *et al.*, 2024).  
223 The mechanisms of the winter increase in disease prevalence remains unclear and may involve  
224 seasonal changes in temperature, bacterial communities, or host condition. Notably, diseased  
225 individuals were not restricted to winter; 5–10% of urchins showed a diseased condition even in  
226 summer. However, *D. yoshimurai* densities were low in summer on both diseased and healthy urchins,  
227 implying that the symbiont’s abundance is not simply driven by whether the host is diseased or not.  
228 Instead, the seasonal density pattern appears to be shaped by the interaction between host disease  
229 dynamics and the amphipod’s own reproductive schedule, with high densities in winter arising when  
230 newly recruited juveniles encounter abundant diseased hosts.

231 Based on the CPUE data, urchin availability (as a proxy for local density) was stable both  
232 seasonally and interannually (Fig. 2). The size structure of urchins was likewise stable across months  
233 and years (Fig. 4). Moreover, test diameter was broadly similar among individuals with and without  
234 visible lesions and with and without *D. yoshimurai* (Fig. 3). Although diseased urchins tended to be  
235 only marginally larger, there was no consistent tendency for urchins hosting *D. yoshimurai* to be  
236 larger or smaller than those without *D. yoshimurai* (Fig. 3). Overall, host density and host size were  
237 generally stable across categories and over time, and are therefore unlikely to be major drivers of the  
238 seasonal patterns described in this study.

239 Body-length data of *D. yoshimurai* showed that juveniles (<2.5 mm) occurred on diseased  
240 urchins throughout the year but were especially abundant in winter and early spring, forming distinct  
241 peaks in the smallest size classes (Fig. 4). Size–frequency distributions often overlapped among  
242 months and did not consistently show smooth shifts in mode. Although clear modal progression of  
243 cohorts was not always evident, the recurring pulses of small juveniles in winter strongly suggest that  
244 recruitment is concentrated in this season. Ovigerous females, in contrast, were rare overall: only

245 seven were recorded from diseased urchins and five from healthy urchins across the entire study  
246 period. They were most frequently observed in late summer and early autumn on both host types. The  
247 small number of ovigerous females prevents a definitive determination of the reproductive season,  
248 but the temporal combination of (i) ovigerous females and large mature females in late summer–  
249 autumn and (ii) juvenile pulses in winter is consistent with reproduction peaking in late summer to  
250 autumn and recruitment continuing into winter. At the same time, the detection of small juveniles  
251 throughout the year, including summer months when overall densities were low, suggests that some  
252 level of reproduction may occur year-round, albeit at much reduced intensity outside this apparent  
253 peak.

254 Marked differences in size structure between diseased and healthy hosts point to strong  
255 ontogenetic variation in habitat use. Diseased urchins were overwhelmingly dominated by juveniles  
256 in most months, whereas the smaller assemblages on healthy urchins often contained a relatively  
257 higher proportion of adults, including ovigerous females (Figs. 4, 5). This pattern suggests that  
258 diseased urchins, and their diseased areas in particular, serve as especially important habitat for early  
259 life stages. Juvenile recruitment appears to occur mainly in winter, when disease prevalence is high,  
260 and juveniles may preferentially occupy lesions rather than the intact surfaces of healthy urchins. In  
261 contrast, healthy urchins hosted only small numbers of juveniles, particularly in summer (Figs. 6, 7).  
262 This suggests that healthy urchins are likely used only opportunistically, mainly during winter  
263 recruitment peaks, when juvenile abundance increases and individuals may spill over from lesions  
264 onto alternative substrates.

265 It is also striking that many diseased urchins hosted numerous juveniles but no large adults, and  
266 that ovigerous females were rare on both diseased and healthy hosts despite intensive sampling (348  
267 urchins and 1,899 amphipods in total). One possibility is that *S. intermedius* is not the main  
268 reproductive habitat for *D. yoshimurai* and that a substantial fraction of reproduction occurs on other  
269 echinoid hosts or alternative substrates in the surrounding habitat (cf. Vader, 1978; Bousfield &  
270 Hendrycks, 1995). The frequent occurrence of urchins bearing only juveniles is consistent with  
271 substantial host-to-host movement, although our data cannot distinguish between local reproduction  
272 on a given host and immigration of juveniles from elsewhere.

273 The reason why *D. yoshimurai* aggregates so clearly on diseased urchins, particularly as  
274 juveniles, remains unresolved. Two non-exclusive hypotheses have been proposed to explain this  
275 behaviour: (1) amphipods aggregate on diseased areas to feed on exposed host tissues, and (2)  
276 diseased areas provide shelter from host defences such as pedicellariae (Kodama *et al.*, 2020, 2024).  
277 DNA metabarcoding of gut contents has shown that urchin-derived material constitutes only a minor  
278 fraction of the diet of *D. yoshimurai*, even for individuals collected from lesions, whereas sediments

279 and other non-host resources dominate (Kodama *et al.*, 2024). This evidence partially refutes the idea  
280 that feeding on host tissue is the primary driver of aggregation. Considering that juveniles are smaller  
281 and likely more vulnerable to physical disturbance and host defensive structures, it seems plausible  
282 that lesions function mainly as relatively safe microhabitats where pedicellariae are absent or reduced,  
283 and where fine sediments and biofilms accumulate. Under this scenario, diseased urchins provide  
284 structurally favourable patches for juveniles, while adults can utilize a broader set of microhabitats  
285 on both diseased and healthy hosts.

286 More broadly, *D. yoshimurai* exemplifies how a symbiotic amphipod can exploit host pathology  
287 as a key habitat feature within its life history. Amphipods of the genus *Dactylopleustes* are widely  
288 recognised as echinoid symbionts and have evolved morphological traits suited for living on urchin  
289 surfaces (Vader, 1978; Bousfield & Hendrycks, 1995; Tomikawa *et al.*, 2004). Our results show that,  
290 at least for *D. yoshimurai*, this association is further shaped by the occurrence of disease lesions that  
291 appear and disappear seasonally on the host. Such disease- and condition-mediated changes in habitat  
292 quality may not be unique to echinoid–amphipod associations. In other echinoids, bald sea urchin  
293 disease and related pathologies produce conspicuous test lesions that are colonized by dense and  
294 distinctive bacterial communities, distinct from those on surrounding healthy tissues (Becker *et al.*,  
295 2008; Shaw *et al.*, 2023; Carella *et al.*, 2025). These lesions and spineless patches can also be  
296 overgrown by macro-epibionts such as encrusting bryozoans (Queiroz *et al.*, 2020). Moreover,  
297 epibionts living on echinoid spines and tests act as important biotic substrates that strongly influence  
298 the richness and composition of associated sessile assemblages (Hétérier *et al.*, 2008; Linse *et al.*,  
299 2008; Rodríguez-Barreras *et al.*, 2023), and in some cases can even alter host physiological responses  
300 (Queiroz *et al.*, 2020). Similar links between host condition and associated fauna are well documented  
301 in corals, where disease lesions can be selectively exploited by corallivores and where the diversity  
302 and abundance of coral-associated invertebrates depend strongly on the persistence and health of live  
303 coral hosts (Stella *et al.*, 2011; Montano 2020, 2022). Taken together, these examples suggest that the  
304 strong coupling we observed between host disease status and *D. yoshimurai* abundance is one instance  
305 of a broader pattern in which host pathology and condition structure the ecological opportunities  
306 available to associated fauna.

307 CPUE varied little over time (Fig. 2b), suggesting that the disease producing lesions recurs  
308 seasonally but is not severe enough to cause a major decline in the local urchin population. This  
309 coexistence with a moderate disease burden is likely important for *D. yoshimurai*, since a stable host  
310 population can provide a recurrent supply of lesioned microhabitats from year to year. A disease  
311 severe enough to substantially reduce host density would be unlikely to sustain a symbiont that  
312 depends on lesions as a key habitat, except for short-lived opportunistic use.

313        From the host's perspective, however, the net effect of *D. yoshimurai* remains uncertain.  
314        Although gut-content metabarcoding indicates that the amphipod does not rely heavily on host tissues  
315        for food (Kodama *et al.*, 2024) and is therefore unlikely to be a primary cause of lesion formation,  
316        dense aggregations on lesions could still influence wound healing and local microbial communities,  
317        potentially modifying the trajectory of bald sea urchin disease. Disentangling whether *D. yoshimurai*  
318        ultimately mitigates, exacerbates, or is largely neutral with respect to disease progression will require  
319        experimental manipulations of amphipod density and lesion presence on infected urchins.

320        In summary, this study demonstrates that the population dynamics of *D. yoshimurai* on *S. intermedius* are jointly structured by host disease status and the amphipod's life history. Diseased  
321        urchins, especially in winter when bald disease is most prevalent, provide critical habitat for juvenile  
322        recruitment and growth, whereas healthy urchins support lower densities but are used by all life stages,  
323        including ovigerous females. Reproduction appears to peak in late summer to autumn with  
324        recruitment continuing into winter, and some level of reproduction likely occurs year-round. These  
325        findings highlight the importance of considering host disease status when evaluating the ecology of  
326        symbionts and suggest that changes in the frequency or severity of urchin diseases, regardless of  
327        whether they are driven by environmental change or by other factors, could have cascading effects  
328        on associated amphipod communities. Future work combining experimental manipulations of lesion  
329        availability, direct observations of host switching and movement, and further dietary and microbiome  
330        analyses will be essential to clarify the functional role of the aggregation of *D. yoshimurai* on the  
331        disease lesions of *S. intermedius*.

333

334

335        ■ **Acknowledgements**

336        We gratefully acknowledge Masaaki Hirano, Takanori Suzuki, Naoya Ohtsuchi, and the other  
337        members of OCRC for supporting samplings in Otsuchi Bay. We thank Tomohiko Kawamura (The  
338        University of Tokyo) for providing helpful comments that improved the study. This study was  
339        supported by grants-in-aid from the Mikimoto Fund for Marine Ecology, Japan. This study was also  
340        partly supported by the Tohoku Ecosystem-Associated Marine Sciences project, and Cooperative  
341        Research (No. 117: Apr 2023-Mar 2024) of Atmosphere and Ocean Research Institute, The University  
342        of Tokyo.

343

344

345        ■ **Statements and Declarations**

346 **Author Contributions statement**

347 MK, RY, and JH conceptualized and designated this study. JH and MK conducted sample collections.  
348 KT made a reliable identification of our specimens of *Dactylopleustes yoshimurai*, which had been  
349 originally described by KT. MK, RY, and JH carried out all the sample processing. MK and RY carried  
350 out data processing and statistical analyses. JH, GK, and TK supervised interpretations for the results.  
351 MK wrote the manuscript and made figures with support from RY and JH. KT, GK, and TK critically  
352 reviewed the manuscript and provided substantial input. All the authors checked the manuscript and  
353 gave their approval for the final version for submission.

354

355 **Funding**

356 This study was supported by grants-in-aid from the Mikimoto Fund for Marine Ecology, Japan. This  
357 study was also partly supported by the Tohoku Ecosystem-Associated Marine Sciences project, and  
358 Cooperative Research (No. 117: Apr 2023-Mar 2024) of Atmosphere and Ocean Research Institute,  
359 The University of Tokyo.

360

361 **Data availability**

362 The data underlying this article will be shared on reasonable request to the corresponding author.

363

364 **Ethical approval**

365 All applicable international, national and/or institutional guidelines for sampling, care and  
366 experimental use of organisms for the study have been followed and all necessary approvals have  
367 been obtained. The study did not involve human participants. No animal welfare approval was  
368 required as we were working with common invertebrates.

369

370 **Conflict of interest**

371 The authors declare that they have no competing interests.

372

373

374 **■ Literature cited**

375 Becker, P. T., Egea, E. & Eeckhaut, I., 2008. Characterization of the bacterial communities associated  
376 with the bald sea urchin disease of the echinoid *Paracentrotus lividus*. *Journal of Invertebrate  
377 Pathology*, 98: 136–147.

378 Bousfield, E. L. & Hendrycks, E. A., 1995. The amphipod family Pleustidae on the Pacific Coast  
379 North America. Part III. Subfamilies parapleustinae, Dactylopleustinae, and Pleusirinae:

380 Systematics and distributional ecology. *Amphipacifica*, 2: 65–133.

381 Carella, F., Correggia, M., Cordone, A., Iacovino, O., Maresca, F., Villari, G., Roque, A. & De Vico,  
382 G., 2025. Bald disease in a natural population of the purple sea urchin *Paracentrotus lividus* of  
383 the Mediterranean Sea: from spines to tissues. *Journal of Invertebrate Pathology*, 213: 108415.  
384 <https://doi.org/10.1016/j.jip.2025.108415>

385 Hanaoka, T., Goto, R., Nakajima, H. & Kodama, M., 2025. A new species of the genus *Leucothoe*  
386 Leach, 1814 (Crustacea: Amphipoda: Leucothoidae) associated with a limid bivalve from  
387 Sugashima Island, Japan. *Zootaxa*, 5696: 567–589.  
388 <https://doi.org/10.11646/zootaxa.5696.4.6>

389 Horton, T., Lowry, J. K., De Broyer, C., Bellan-Santini, D., Copilaş-Ciocianu, D., Corbari, L.,  
390 Costello, M. J., Daneliya, M. E., Dauvin, J. C., Fišer, C., Gasca, R., Grabowski, M., Guerrra-  
391 García, J. M., Hendrycks, E. A., Hughes, L. E., Jaume, D., Jazdzewski, K., Kim, Y. H., King, R.,  
392 Krapp-Schickel, T., LeCroy, S. E., Lörz, A. N., Mamos, T., Senna, A. R., Serejo, C. S., Souza-  
393 Filho, J. F., Tandberg, A. H. S., Thomas, J. D., Thurston, M., Vader, W., Väinölä, R., Valls  
394 Domedel, G., Vonk, R., White, K. N. & Zeidler, W., 2025. World Amphipoda Database. (URL:  
395 <https://www.marinespecies.org/amphipoda>) Accessed on 23 December 2025.  
396 <https://doi.org/10.14284/368>

397 Iwasa-Arai, T. & Serejo, C. S., 2018. Phylogenetic analysis of the family cyamidae (Crustacea:  
398 Amphipoda): a review based on morphological characters. *Zoological Journal of the Linnean  
399 Society*, 184(1): 66–94.  
400 <https://doi.org/10.1093/zoolinnean/zlx101>

401 Johnson, P. T., 1971. Studies on diseased urchins from Point Loma. In: W. J. North, (ed.), Kelp habitat  
402 improvement project, annual report, 1970–1971, California Institute of Technology, Pasadena,  
403 pp. 82–90.

404 Hétérier, V., David, B., De Ridder, C. & Rigaud, T., 2008. Ectosymbiosis is a critical factor in the  
405 local benthic biodiversity of the Antarctic deep sea. *Marine Ecology Progress Series*, 364: 67–  
406 76.  
407 <https://doi.org/10.3354/meps07487>

408 Kodama, M., Hayakawa J. & Kawamura, T., 2020. Aggregations of *Dactyloblestes* (Amphipoda:  
409 Pleustidae) on the diseased areas of the host sea-urchin, *Strongylocentrotus intermedius*. *Marine  
410 Biodiversity*, 50(4): 62.  
411 <https://doi.org/10.1007/s12526-020-01100-9>

412 Kodama, M., White, K. N., Hosoki, T. K. & Yoshida, R., 2022. Leucothoid amphipod and terebellid  
413 polychaete symbiosis with description of a new species of *Leucothoe* Leach, 1814 (Crustacea:

414 Amphipoda: Leucothoidae). Systematics and Biodiversity, 20; 2118389.  
415 <https://doi.org/10.1080/14772000.2022.2118389>

416 Kodama, M., Yamazaki, R., Hayakawa, J., Murata, G., Tomikawa, K., Kawamura, T., Kume, G. &  
417 Kobari, T., 2024. Feeding ecology of the urchin symbiont *Dactylopleustes yoshimurai*  
418 (Amphipoda) revealed by DNA metabarcoding. Marine Biology, 171: 190.  
419 <https://doi.org/10.1007/s00227-024-04507-1>

420 Linse, K., Walker, L. J. & Barnes, D. K. A., 2008. Epizoic communities on Antarctic cidaroid  
421 echinoids. Antarctic Science, 20: 227–244.  
422 <https://doi.org/10.1017/S0954102008001181>

423 Lowry, J. K. & Myers, A. A., 2017. A phylogeny and classification of the Amphipoda with the  
424 establishment of the new order Ingolfiellida (Crustacea: Peracarida). Zootaxa, 4265(1): 1–89.  
425 <https://doi.org/10.11646/zootaxa.4265.1.1>

426 Montano, S., 2020. The extraordinary importance of coral-associated fauna. Diversity, 12: 357.  
427 <https://doi.org/10.3390/d12090357>

428 Montano, S., 2022. Diversity of coral-associated fauna: an urgent call for research. Diversity, 14: 765.  
429 <https://doi.org/10.3390/d14090765>

430 Queiroz, E. T., Bronstein, O., Ben-Dov, E., Rothman, S. B., Barutski, F., Wuthrich, D., Geyer, R.,  
431 Ribeiro, S. M., Migotto, A. E. & Bianchini, A., 2020. An unprecedented association of an  
432 encrusting bryozoan on the test of a live sea urchin. Marine Biodiversity, 50: 86.  
433 <https://doi.org/10.1007/s12526-020-01108-1>

434 Rodríguez-Barreras, R., Dominicci-Maura, A., Tosado-Rodríguez, E. L. & Godoy-Vitorino, F., 2023.  
435 The epibiotic microbiota of wild Caribbean sea urchin spines is species specific. Microorganisms,  
436 11: 391.  
437 <https://doi.org/10.3390/microorganisms11020391>

438 Shaw, C. G., Pavloudi, C., Barela Hudgell, M. A., Crow, R. S., Saw, J. H., Pyron, R. A. & Smith, L.  
439 C., 2023. Bald sea urchin disease shifts the surface microbiome on purple sea urchins in an  
440 aquarium. Pathogens and Disease, 81: ftad025.  
441 <https://doi.org/10.1093/femspd/ftad025>

442 Stella, J. S., Pratchett, M. S., Hutchings, P. A. & Jones, G. P., 2011. Coral-associated invertebrates:  
443 diversity, ecological importance and vulnerability to disturbance. Oceanography and Marine  
444 Biology: An Annual Review, 49: 43–104.  
445 <https://doi.org/10.1201/b11009-4>

446 Tomikawa, K., Hendrycks, E. A. & Mawatari, S. F., 2004. A new species of the genus *Dactylopleustes*  
447 (Crustacea: Amphipoda: Pleustidae) from Japan, with a partial redescription of *D. Echinoides*

448 Bousfield and Hendrycks, 1995. Zootaxa, 674: 1–14.  
449 <https://doi.org/10.11646/zootaxa.674.1.1>

450 Tomikawa, K., Yanagisawa, M., Higashiji, T., Yano, N. & Vader, W., 2019. A new species of  
451 podocerus (Crustacea: Amphipoda: Podoceridae) associated with the whale shark *Rhincodon*  
452 *typus*. Species Diversity, 24(2): 209–216.  
453 <https://doi.org/10.12782/specdiv.24.209>

454 Vader, W., 1978. Associations between amphipods and echinoderms. Astarte, 11: 123–134.  
455 Vader, W., 1983. Associations between amphipods (Crustacea) and sea anemones (Anthozoa,  
456 Actiniaria). Memoirs of the Australian Museum, 68: 141–152.

457 Vader, W. & Tandberg, A. H. S., 2013. A survey of amphipods associated with molluscs. Crustaceana,  
458 86(7–8): 1038–1049.  
459 <https://doi.org/10.1163/15685403-00003210>

460 Vader, W. & Tandberg, A. H. S., 2015. Amphipods as associates of other Crustacea: a survey. Journal  
461 of Crustacean Biology, 35(4): 522–532.  
462 <https://doi.org/10.1163/1937240X-00002343>

463

464

465 **Addresses**

466 (MK) (GK) (TK) Faculty of Fisheries, Kagoshima University, 4–50–20 Shimoarata, Kagoshima 890–  
467 0056, Japan

468 (RY) Graduate School of Agriculture, Forestry and Fisheries, Kagoshima University, 4–50–20  
469 Shimoarata, Kagoshima 890–0056, Japan

470 (KT) Graduate School of Humanities and Social Sciences, Hiroshima University, 1-1-1 Kagamiyama,  
471 Higashihiroshima, Hiroshima 739-8524, Japan

472 (JH) Otsuchi Coastal Research Center, Atmosphere and Ocean Research Institute, The University of  
473 Tokyo, 1-19-8 Akahama, Otsuchi 028-1102, Iwate, Japan

474

475 **E-mail address of corresponding author**

476 (MK) [mkodama@fish.kagoshima-u.ac.jp](mailto:mkodama@fish.kagoshima-u.ac.jp)

477

478 **Figure legends**

479 Fig. 1. Map showing the study site in Otsuchi Bay, Japan.

480

481 Fig. 2. (a) Seasonal fluctuation in the proportion (%) of *Strongylocentrotus intermedius* individuals  
482 bearing *Dactylobleustes yoshimurai* (red) and the proportion (%) showing disease symptoms of  
483 “bald urchin disease” (black) at Akahama, Otsuchi Bay, from Jan 2020 to Jan 2024 (n = 50  
484 urchins examined per survey). (b) Seasonal fluctuation in the catch per unit effort (CPUE;  
485 individuals h<sup>-1</sup>) of *S. intermedius* during monthly SCUBA surveys. CPUE was calculated as 50  
486 individuals divided by the elapsed time (h) required to locate and measure 50 urchins; higher  
487 values indicate greater local availability of urchins. Plots are missing for months without surveys  
488 and for months in which CPUE could not be calculated (e.g., due to missing end-time records).  
489 Grey vertical bands indicate winter (Dec–Feb).

490

491 Fig. 3. Test diameter (mm) of *Strongylocentrotus intermedius* for healthy (no visible lesion) and  
492 diseased (with visible lesion) individuals with or without visible *Dactylobleustes yoshimurai*.  
493 Boxes represent the lower and upper quartiles. Black bold line in each box indicates the median.  
494 Whiskers extend to the most extreme values within 1.5× the interquartile range; values beyond  
495 this range are treated as outliers. Grey jittered dots indicate individual urchins. Letters (a, b, and  
496 ab) denote significant differences among groups (Dunn’s test with Bonferroni correction,  $\alpha =$   
497 0.05).

498

499 Fig. 4. Monthly size–frequency distributions of *Strongylocentrotus intermedius* between Jan 2020  
500 and Jan 2024 (50 individuals per survey month). Histograms show test diameter (mm) and are  
501 colour-coded by with/without visible lesion and with/without visible *Dactylobleustes*  
502 *yoshimurai*. Panels are absent for unsurveyed months (Jul 2020, Oct 2021; Nov, Dec 2022; Feb,  
503 Nov 2023).

504

505 Fig. 5. Seasonal fluctuation in the number of *Dactylobleustes yoshimurai* (number of individuals per  
506 host urchin) on diseased (red) and healthy (black) *Strongylocentrotus intermedius* from Jan 2021  
507 to Jan 2024. Points indicate observed counts for individual hosts (six diseased and six healthy  
508 urchins collected per survey). Solid curves show fitted lines from generalized additive models,  
509 with shaded bands indicating 95% confidence intervals. Grey vertical bands indicate winter  
510 (Dec–Feb).

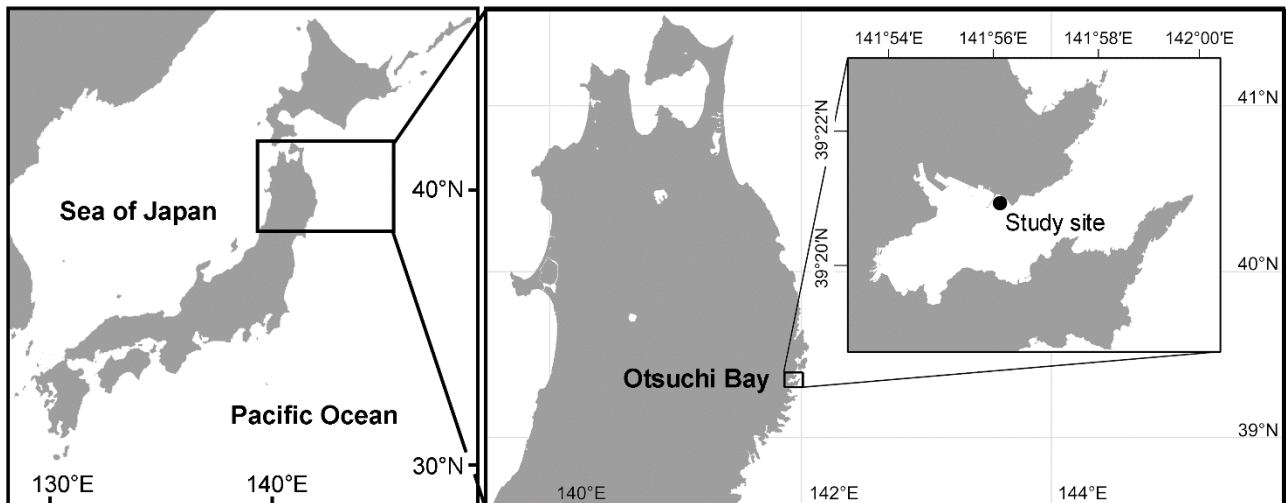
511

512 Fig. 6. Monthly size–frequency distributions of *Dactylopleustes yoshimurai* collected from diseased  
513 *Strongylocentrotus intermedius* between Jan 2021 and Jan 2024 (six hosts per survey month).  
514 Histograms show body length (mm) and are colour-coded by sex and developmental stage  
515 (juveniles, immature females, mature females, ovigerous females, and males). Arrows indicate  
516 ovigerous females. Panels are absent for unsampled months (Oct 2021; Apr, Nov, Dec 2022; Feb,  
517 Jun, Aug, Nov 2023), whereas empty panels (Aug 2022, Jul 2023) indicate months that were  
518 sampled but yielded no amphipods.

519

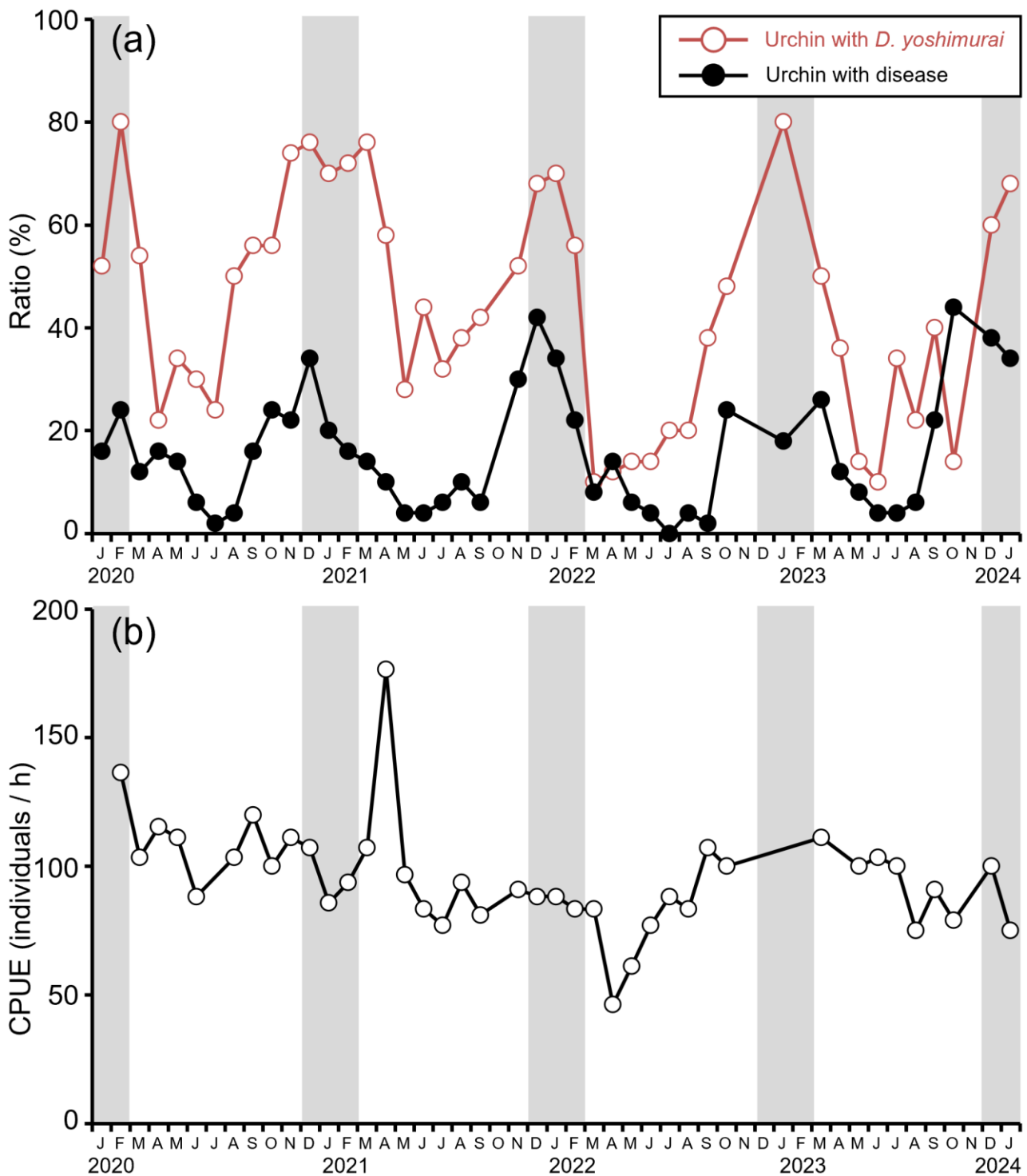
520 Fig. 7. Monthly size–frequency distributions of *Dactylopleustes yoshimurai* collected from healthy  
521 *Strongylocentrotus intermedius* between Jan 2021 and Jan 2024 (six hosts per survey month).  
522 Histograms show body length (mm) and are colour-coded by sex and developmental stage  
523 (juveniles, immature females, mature females, ovigerous females, and males). Arrows indicate  
524 ovigerous females. Panels are absent for unsampled months (Oct 2021; Apr, Nov, Dec 2022; Feb,  
525 Jun, Aug, Nov 2023), whereas empty panels (Sep, Oct 2023) indicate months that were sampled  
526 but yielded no amphipods.

527



528  
529  
530  
531  
532

Fig. 1. Map showing the study site in Otsuchi Bay, Japan.



533

534

535

536

537

538

539

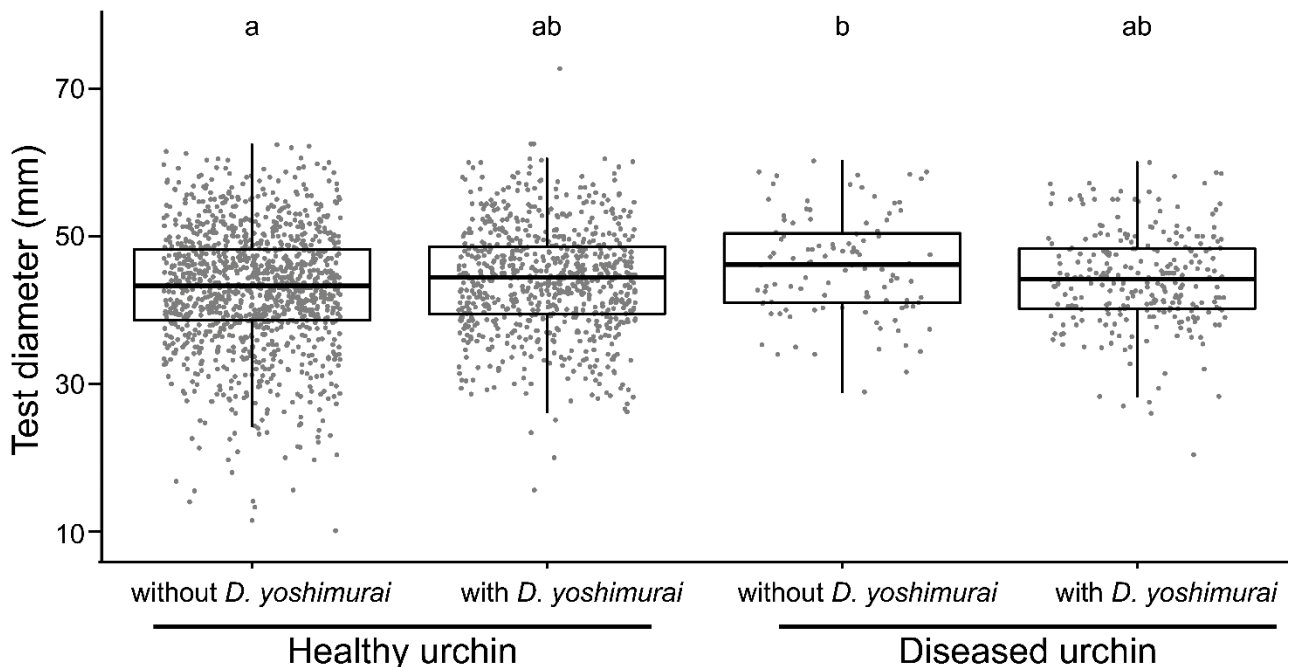
540

541

542

543

Fig. 2. (a) Seasonal fluctuation in the proportion (%) of *Strongylocentrotus intermedius* individuals bearing *Dactylobleustes yoshimurai* (red) and the proportion (%) showing disease symptoms of “bald urchin disease” (black) at Akahama, Otsuchi Bay, from Jan 2020 to Jan 2024 ( $n = 50$  urchins examined per survey). (b) Seasonal fluctuation in the catch per unit effort (CPUE; individuals  $h^{-1}$ ) of *S. intermedius* during monthly SCUBA surveys. CPUE was calculated as 50 individuals divided by the elapsed time (h) required to locate and measure 50 urchins; higher values indicate greater local availability of urchins. Plots are missing for months without surveys and for months in which CPUE could not be calculated (e.g., due to missing end-time records). Grey vertical bands indicate winter (Dec–Feb).



544  
545 Fig. 3. Test diameter (mm) of *Strongylocentrotus intermedius* for healthy (no visible lesion)  
546 and diseased (with visible lesion) individuals with or without visible *Dactylobleustes yoshimurai*. Boxes  
547 represent the lower and upper quartiles. Black bold line in each box indicates the median. Whiskers  
548 extend to the most extreme values within  $1.5 \times$  the interquartile range; values beyond this range are  
549 treated as outliers. Grey jittered dots indicate individual urchins. Letters (a, b, and ab) denote  
550 significant differences among groups (Dunn's test with Bonferroni correction,  $\alpha = 0.05$ ).  
551

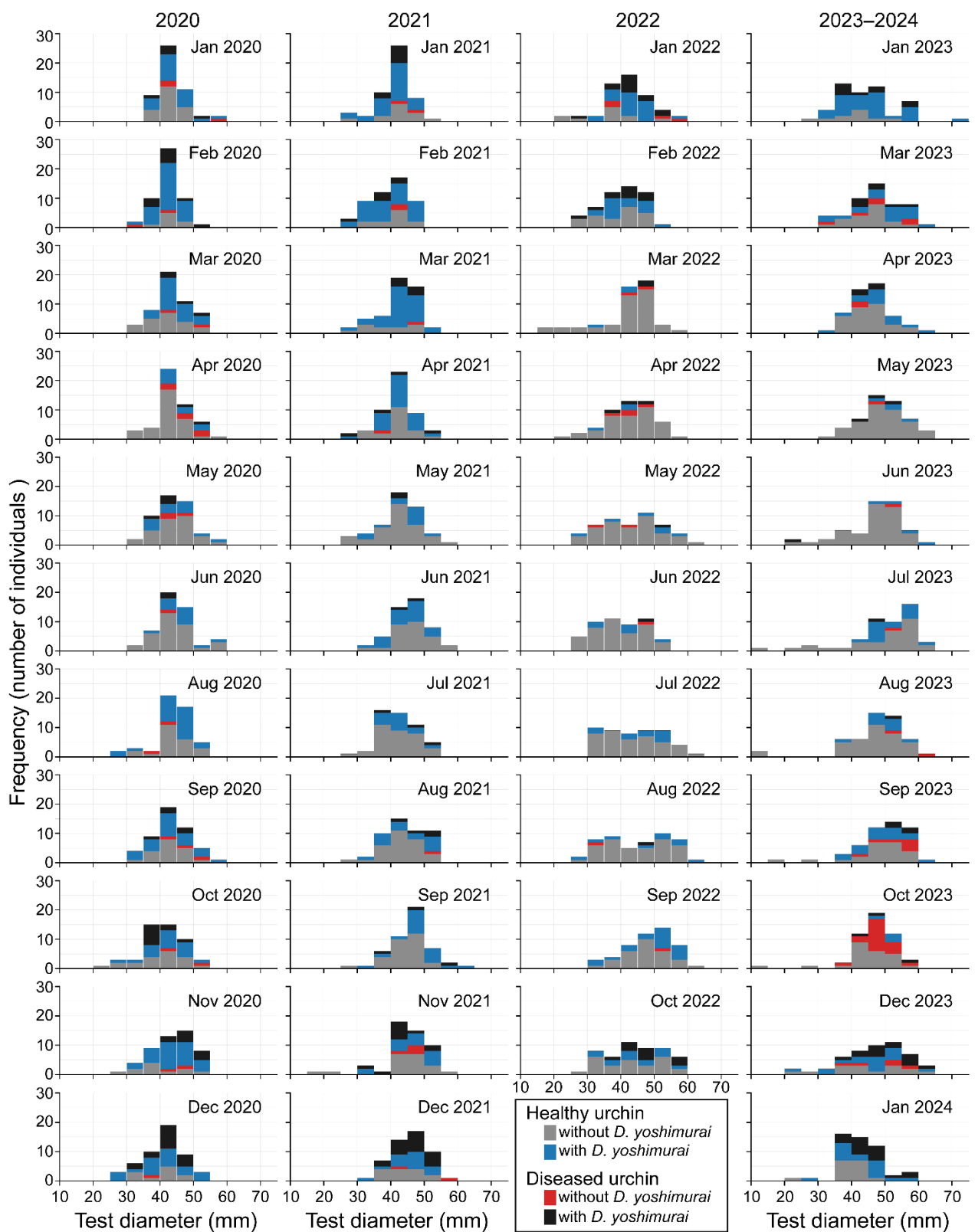
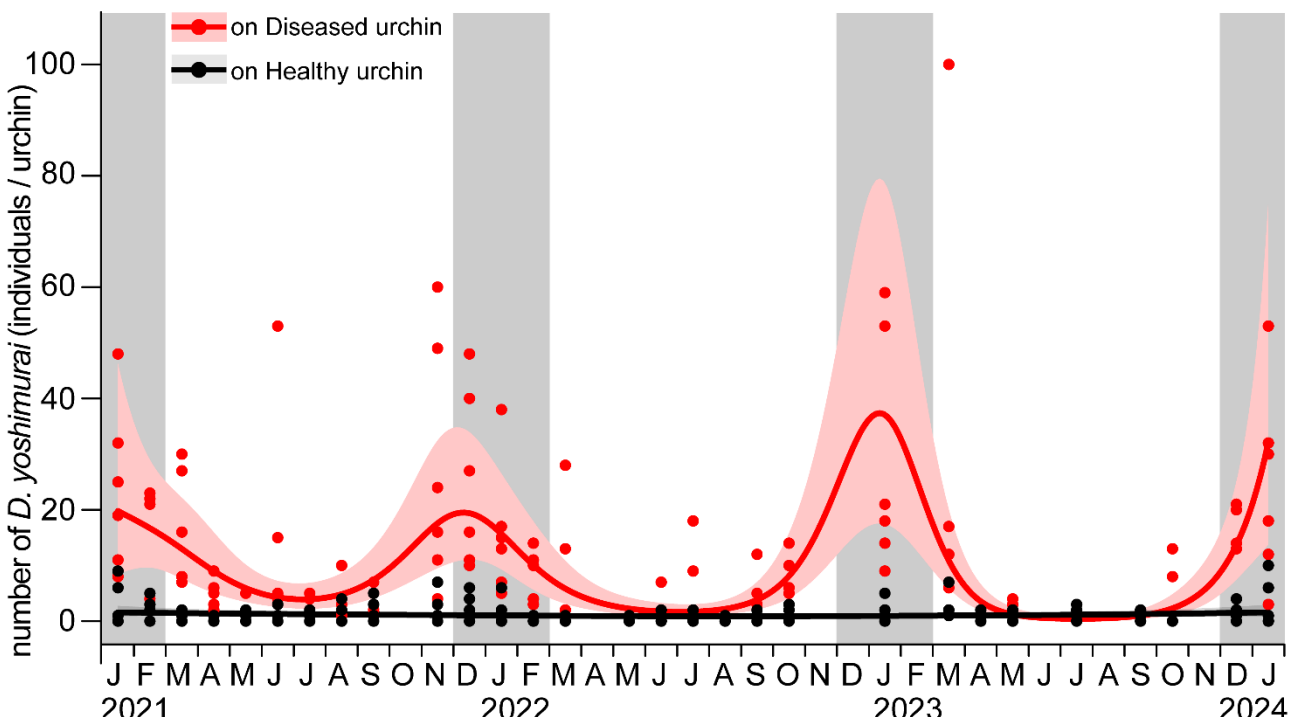
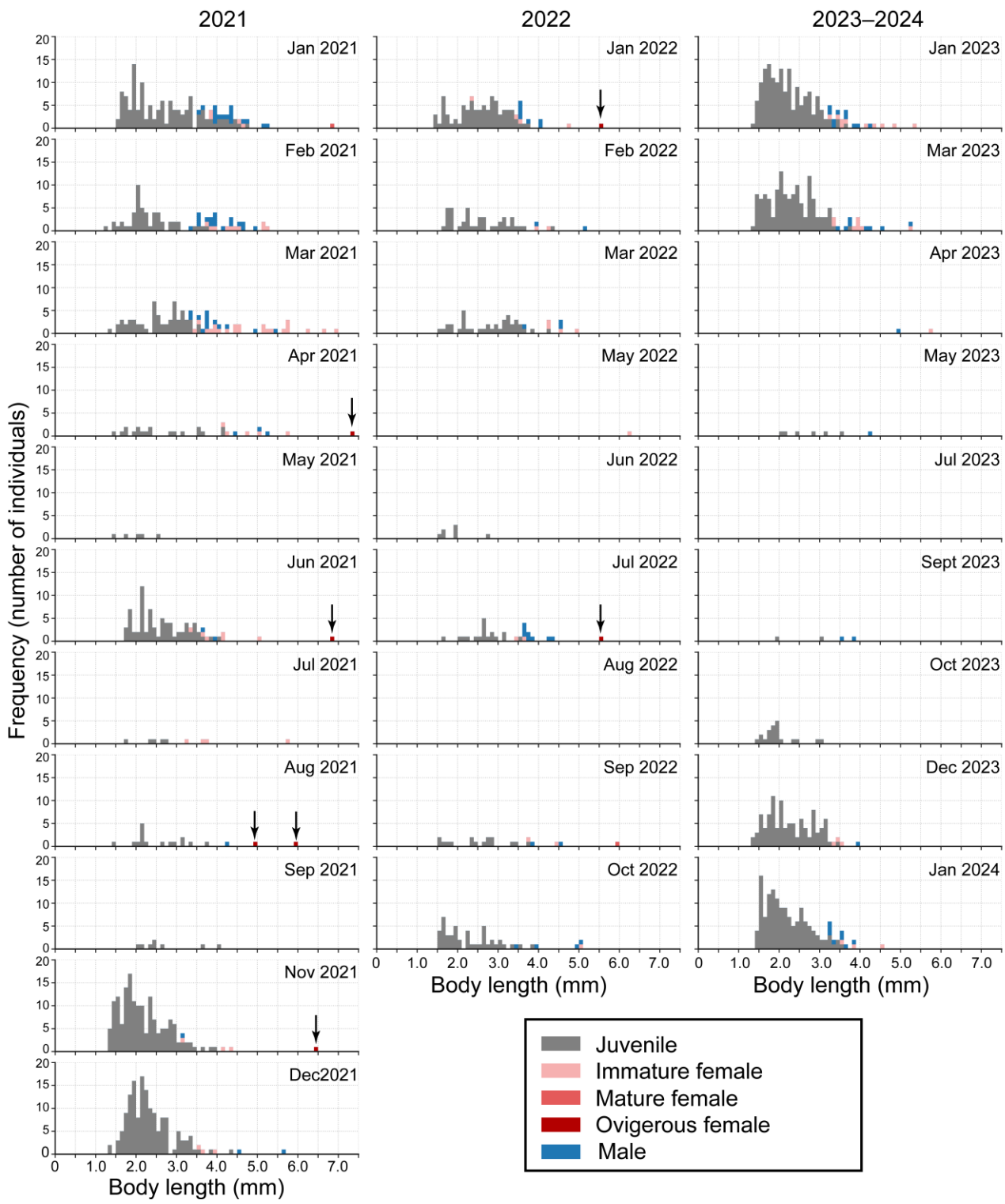


Fig. 4. Monthly size-frequency distributions of *Strongylocentrotus intermedius* between Jan 2020 and Jan 2024 (50 individuals per survey month). Histograms show test diameter (mm) and are colour-coded by with/without visible lesion and with/without visible *Dactylopleustes yoshimurai*. Panels are absent for unsurveyed months (Jul 2020, Oct 2021; Nov, Dec 2022; Feb, Nov 2023).



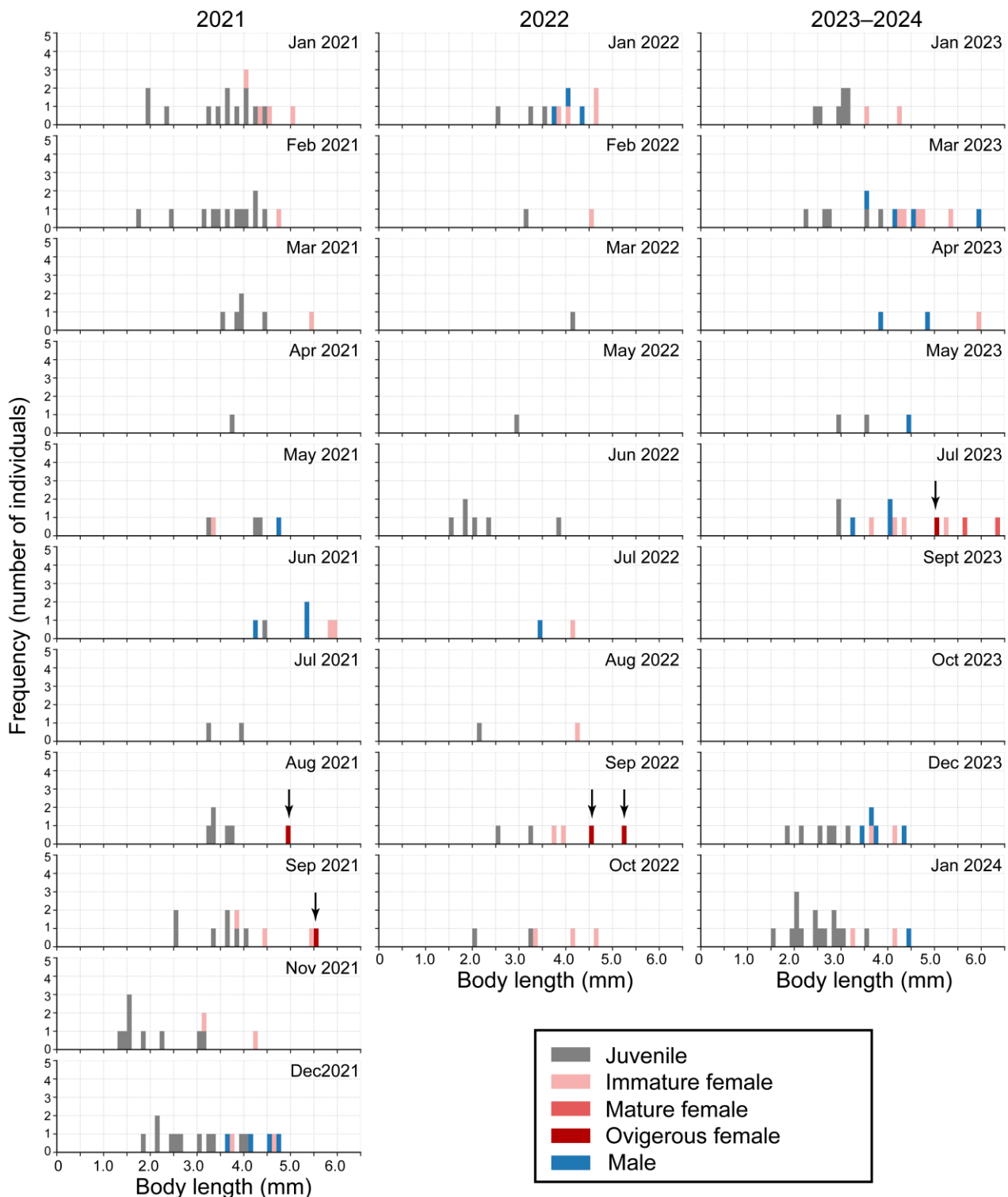
559  
560 Fig. 5. Seasonal fluctuation in the number of *Dactylobleustes yoshimurai* (number of individuals per  
561 host urchin) on diseased (red) and healthy (black) *Strongylocentrotus intermedius* from Jan 2021 to  
562 Jan 2024. Points indicate observed counts for individual hosts (six diseased and six healthy urchins  
563 collected per survey). Solid curves show fitted lines from generalized additive models, with shaded  
564 bands indicating 95% confidence intervals. Grey vertical bands indicate winter (Dec–Feb).  
565  
566  
567



568  
569

570 Fig. 6. Monthly size–frequency distributions of *Dactylopleustes yoshimurai* collected from diseased  
571 *Strongylocentrotus intermedius* between Jan 2021 and Jan 2024 (six hosts per survey month).  
572 Histograms show body length (mm) and are colour-coded by sex and developmental stage (juveniles,  
573 immature females, mature females, ovigerous females, and males). Arrows indicate ovigerous  
574 females. Panels are absent for unsampled months (Oct 2021; Apr, Nov, Dec 2022; Feb, Jun, Aug, Nov  
575 2023), whereas empty panels (Aug 2022, Jul 2023) indicate months that were sampled but yielded no  
576 amphipods.

577



578  
579

580 Fig. 7. Monthly size-frequency distributions of *Dactylopleustes yoshimurai* collected from healthy  
581 *Strongylocentrotus intermedius* between Jan 2021 and Jan 2024 (six hosts per survey month).  
582 Histograms show body length (mm) and are colour-coded by sex and developmental stage (juveniles,  
583 immature females, mature females, ovigerous females, and males). Arrows indicate ovigerous  
584 females. Panels are absent for unsampled months (Oct 2021; Apr, Nov, Dec 2022; Feb, Jun, Aug, Nov  
585 2023), whereas empty panels (Sep, Oct 2023) indicate months that were sampled but yielded no  
586 amphipods.  
587